Letter

Electrostatic tapering for efficient generation of radiation

Miron Voin [*] and Levi Schächter [†]
Department of Electrical and Computer Engineering Technion—Israel Institute of Technology Haifa 32000, Israel

(Received 27 September 2021; accepted 26 January 2022; published 9 February 2022)

We demonstrate the feasibility of electrostatic (dc) tapering such that the net average force of the electromagnetic (ac) field is compensated by a dc field, which at resonance may be interpreted as "direct" energy transfer from the dc to the ac field. This combination persists in all three components of the setup—e-gun, resonant zone, and collector, in each one playing a different role. In equilibrium, the two field components field-emit at the cathode a density modulated cylindrical beam which is accelerated along the e-gun by the dc field; the latter also focuses the e-beam. Radiation confinement perpendicular to the e-beam is ensured by an array of dielectric Bragg-mirrors and an array of metallic hollow electrodes impose synchronous bunches and wave. This double periodic structure ensures the coexistence of dc and ac fields in the same volume. Numerical simulations demonstrate the feasibility of generation of order of 1[W] power at 1 THz from a volume on a scale of few mm^3 with efficiency of the order of 25%.

DOI: 10.1103/PhysRevE.105.L023201

High-efficiency radiation sources such as traveling wave tubes, gyrotrons, and free electron lasers are of great demand in a large verity of fields in physics, medicine, biology, and chemistry. In all these devices the high efficiency is achieved by adapting (tapering) the local velocity of the electron to the phase velocity of the interacting field. In all these cases, the tapering is achieved by varying the parameters which control the phase velocity of the interacting wave. For example in the case of free-electron laser the period and/or the intensity of the wiggler are changed such that the ponderomotive force's velocity equals the longitudinal velocity of the electron—this is the resonance condition [1]. In this Letter we show that resonance can be maintained by a dc field which can coexist with ac field of the wave. The concept seems to have significant advantages for generation of THz radiation and as such, next we briefly review the needs and the alternatives.

Terahertz frequency band, occupying the boundary between microwave and optical radiation, is of increasing interest for wide scientific and technological community during recent decades [2–5]. Unique properties of this band such as relatively short wavelength with photon energy still lower than a band-gap for common dielectric materials, may be of great interest in telecommunication [6], medicine and biology [7], nondestructive testing [8], security [9], and pollution and global warming monitoring [5]. The same properties make efficient generation of the terahertz radiation challenging and the band is commonly considered as a "gap" in the range of radiation sources.

Generation of THz radiation was proven to be feasible relying on two completely different approaches: On the one hand, the group of devices that employ microelectronics technology consisting, among others, quantum cascade lasers [10], field-effect [11], bipolar transistors [12], and other solid-state paradigms [5,13]. Common to all is the fact, that the interaction of the electrons with the electromagnetic field occurs in solid-state material—we shall refer to these as the solid-state device (SSD). On the other hand, in the second group, the energy exchange occurs in vacuum and we refer to it as vacuum tube device (VTD) [4,14–16]. While the former is very compact as it relies on photolithography, the power and the efficiency are fairy low—typically on a scale of mW of power and 1% or less efficiency. The VTD, can generate high power levels at very high frequencies and high efficiencies. Unfortunately, they are anything but compact.

The description of the model used to demonstrate the new concept in this study, will be accomplished in three steps assuming that steady-state operation has been reached:

(i) All three main components (of azimuthal symmetry), the e-gun, the interaction region, and the collector, occupy one space—see configuration of the device under consideration shown schematically in Fig. 1. Carbon-nanotube (CNT) [17,18] cathode, exposed to a combination of dc and ac (THz) field, field-emits density-modulated electron beam [19,20]. Due to the strong nonlinearity of the Fowler-Nordheim (FN) field-emission process [21], the emitted e-beam has a Gaussian-like longitudinal profile [22,23]. Each emitted microbunch is accelerated primarily by the dc field to velocity synchronous with that of the ac wave. We refer to this region as the *acceleration zone* (AZ).

(ii) Along the *resonance zone* (RZ) the bunch and the wave are designed to be synchronous since any microbunch deceleration associated with the wave amplification, is compensated by the dc field. In other words, in its frame of reference, the bunch experiences, on average, a *zero* net field. The bunch is rapidly decelerated in the *deceleration zone* (DZ).

(iii) To facilitate the coexistence of the dc and ac fields in the same volume we designed an array of thin metallic and

[*] mironv@campus.technion.ac.il
[†] levi@ee.technion.ac.il

 ©2022 American Physical Society

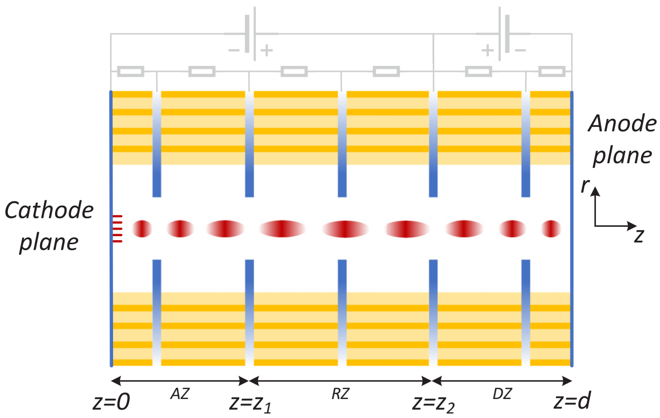

FIG. 1. Schematic representation of the configuration being considered (axial cross-section of azimuthally symmetrical geometry), including three interaction zones (not to scale).

hollowed electrodes which establishes the electrostatic potential on axis and at the same time, it controls the phase velocity of the ac wave. *Radial confinement* of the wave is ensured by a radial Bragg-mirror between every two adjacent electrodes [24], assuming that their spacing is smaller than the vacuum wavelength. The electrodes array and the Bragg-mirrors may be conceived as a *double-periodic structure*.

In what follows, we establish the set of quasianalytic equations that determine the field and particles dynamics. We assume that the cathode's emitting area is small on the scale of the wavelength ($A_{\rm cat} \ll \lambda_0^2$). At current levels whereby space-charge effects are negligible e-beam dc focusing is sufficient. When space-charge effects become important an axial magnetic field is necessary to avoid electrons to hit the metallic electrodes. However, applying a very strong magnetic field may preclude beam radial expansion leading to weak coupling since $\beta_{\rm ph} \sim 0.1$.

Total electric field acting on a particle on axis is a superposition of an ac field $E_z^{(\rm ac)}(r=0,z,t) = E_0^{(\rm ac)}(t)\cos(\omega_0 t - kz)$ and a dc field $E_z^{(\rm dc)}(r=0,z) \equiv E_0^{(\rm dc)}(z)$. The ac amplitude varies slowly in time comparing to $\cos\omega_0 t$ and it may be shown (Ref. [25], Sec. 4.3) that considering interaction with a single harmonic and neglecting the reflected wave, differential equation for the ac field amplitude reads

$$\left(\frac{1}{2\tau_{\rm d}} + \frac{d}{dt}\right)E_0^{(\rm ac)} = \frac{ceN}{\frac{1}{2}\varepsilon_0\varepsilon_{\rm int}A_{\rm cat}d}\langle\beta_i(t)\cos[\chi_i(t)]\rangle_i. \quad (1)$$

Equation of motion for the particle is

$$\begin{aligned}\frac{d}{dt}\beta_i(t) &= \frac{-e}{mc}E_z^{(\rm tot)}(r=0,z=z_i,t)\\ &= \frac{-e}{mc}E_0^{(\rm ac)}\cos(\chi_i) + \frac{-e}{mc}E_0^{(\rm dc)}(z_i). \quad (2)\end{aligned}$$

The phase of the ith particle located at $z_i(t)$ is $\chi_i(t) \equiv kz_i(t) - \omega_0 t$ is also assumed to vary slowly. N represents the number of interacting electrons; d is the structure's length; ε_0 denotes the vacuum permittivity and $\varepsilon_{\rm int} \equiv \langle W_{\rm em}^{(\rm ac)}\rangle_t[\frac{1}{2}\varepsilon_0 A_{\rm cat}\int_0^d dz\langle[E_z^{(\rm ac)}(r=0,z,t)]^2\rangle_t]^{-1}$ is an interaction permittivity (Ref. [25], Par. 2.3.3), which is a property of the structure found in our case as a ratio of the total stored EM energy and the (square of the) interacting component of the electromagnetic field in the interaction volume. The effective decay time coefficient $\tau_{\rm d}$ accounts for the global ohm loss and power extracted from the system. Next, we introduce a set of normalized variables and coefficients: $\zeta = z/d$, $\tau = ct/d$, $\beta = \dot{z}/c$, interaction constant $\alpha = e^2Nd/mc^2\varepsilon_0\varepsilon_{\rm int}A_{\rm cat}$, amplitude $a = (ed/mc^2)E$, normalized potential u, such that $du_{\rm dc}/d\zeta = -a_{\rm dc}$, $\Omega = d\omega_0/c$, $K = kd$, and normalized decay coefficient $T_{\rm d} = c\tau_{\rm d}/d$. With this notation, the governing equations are

$$\begin{aligned}\left(\frac{d}{d\tau} + \frac{1}{2T_{\rm d}}\right)a_{\rm ac} &= \alpha\langle\beta_i\cos\chi_i\rangle_i,\\ \frac{d\beta_i}{d\tau} &= -a_{\rm ac}\cos\chi_i - a_{\rm dc}(\zeta_i),\\ \frac{d\chi_i}{d\tau} &= K(\beta_i - \beta_{\rm ph}), \quad (3)\end{aligned}$$

and global energy conservation is readily verified to read

$$\frac{d}{d\tau}\left\langle\frac{1}{2\alpha}|a_{\rm ac}|^2 + \frac{1}{2}\beta_i^2 - u_{\rm dc}(\zeta_i)\right\rangle_i = -\frac{1}{2\alpha T_{\rm d}}|a_{\rm ac}|^2. \quad (4)$$

To get a flavor of the solution of this set of equations, let us employ the so-called resonant particle model. We first consider the stable regime ($d/d\tau = 0$) in the RZ thus, $\beta_i = \beta_{\rm r} = \beta_{\rm ph}$; subscript r indicates resonant conditions. In this regime, any change in amplitude is compensated by the loss term

$$a_{\rm ac} = 2T_{\rm d}\alpha\beta_{\rm r}\cos\chi_{\rm r}, \quad (5)$$

whereas the zero net force on each microbunch implies

$$a_{\rm ac}\cos\chi_{\rm r} + a_{\rm dc,RZ} = 0. \quad (6)$$

Several facts are evident from this simplified version of the model: (i) the ac amplitude is proportional to the number of electrons therefore the process is coherent and it is proportional to the decay coefficient. (ii) The ac field is proportional to the dc field which clearly is a result from the equilibrium condition, Eq. (6). (iii) As the resonant particle's kinetic energy remains constant and assuming e-bunch center of mass close to that particle, the global energy conservation Eq. (4) may be approximated (with assumption of uniform $a_{\rm dc}$) as $\beta_{\rm ph}a_{\rm dc} \approx -|a_{\rm ac}|^2/2\alpha T_{\rm d}$, which may be interpreted as a "direct" energy transfer from dc to ac.

In the remainder, we consider a simplified version of Eq. (3) and the important results are compared quantitatively with the PIC code by CST [26]. The entire device is divided in the three regions mentioned above: AZ, RZ, and DZ (see Fig. 1); in each region, the dc field ($a_{\rm dc,AZ}$, $a_{\rm dc,RZ}$, and $a_{\rm dc,DZ}$) is assumed to be uniform. Let us start with the operation of the *acceleration zone*.

In this zone three main goals must be accomplished: first, the dc and ac have to *extract* in each period of the wave a Gaussian microbunch based on field-emitting cathode [21] consisting of a carbon nanotubes [18,22,23]. The second goal is to boost the energy of the microbunch from zero to that which corresponds to a normalized kinetic energy $\beta_{\rm ph}^2/2$ such that microbunch and the interacting mode will be synchronous. And the third goal, is to ensure that the microbunch has to "slip out of phase." If at the cathode the peak of the

Gaussian was in zero phase with the wave, then at the end of AZ ($\zeta = \zeta_1$) the phase between the two has to be shifted by approximately π such that the wave will decelerate the microbunch.

Both dc and ac values of the field are chosen such that the peak and average currents satisfy the specifications of the device as manifested in the coupling coefficient α and decay coefficient $\mathrm{T_d}$ [Eqs. (3) and (4)]. With these parameters established in a *self-consistent* way, we define the deviation of the particle's velocity from the phase velocity $\delta\beta_i \equiv \beta_i - \beta_{\rm ph}$, thus in the AZ the equation of motion are simplified to read

$$\frac{d}{d\tau}\delta\beta_i = -a_{\rm ac}\left(\cos\chi_i + \frac{a_{\rm dc,AZ}}{a_{\rm ac}}\right), \quad \frac{d\chi_i}{d\tau} = K\delta\beta_i, \tag{7}$$

and the corresponding Hamiltonian $H_{\rm acc} = K\delta\beta_i^2/2 + a_{\rm ac}(\sin\chi_i + \chi_i a_{\rm dc,AZ}/a_{\rm ac})$. The microbunch generated at the cathode should be rapidly accelerated in the AZ, therefore a tradeoff is anticipated: on the one hand, large ratio ($a_{\rm dc,AZ}/a_{\rm ac} \gg 1$) would be desired to minimize the energy spread (and thus reduce emittance), whereas, on the other hand, minimizing this ratio would help avoid breakdown. Since we know that the Hamiltonian is a constant of motion and denoting by $\chi_{\rm r,0}$ the phase of the resonant particle (in vicinity of the Gaussian peak) at the cathode, the $a_{\rm dc,AZ}$ is given by

$$a_{\rm dc,AZ} = \frac{K\beta_{\rm ph}^2/2 - a_{\rm ac}(\sin\chi_{\rm r} - \sin\chi_{\rm r,0})}{\chi_{\rm r} - \chi_{\rm r,0}}. \tag{8}$$

$\chi_{\rm r}$ is the phase of the resonant particle at the output of the AZ (input of the RZ); at the cathode the velocity is assumed to be zero.

Now we focus our attention to the RZ. Substitution of the resonance condition $\cos\chi_{\rm r} = -a_{\rm dc,RZ}/a_{\rm ac}$ into velocity equation leads to a single particle Hamiltonian of the form

$$H_{\rm res} = K\delta\beta_i^2/2 + a_{\rm ac}(\sin\chi_i - \chi_i\cos\chi_{\rm r}), \tag{9}$$

with χ_i related as a canonical coordinate and $\delta\beta_i$ as a canonical momentum. Hamiltonian $H_{\rm res}$ is similar to the one described by Kroll *et al.* in Ref. [27] for free electron lasers and corresponds to a particle moving in potential $V(\chi) \equiv -a_{\rm ac}U(\chi)$. Figure 2(a) shows behavior of the normalized potential $U(\chi) = -\sin\chi + \chi\cos\chi_{\rm r}$.

In the framework of our formulation, a situation whereby the majority of the particles are trapped corresponds to phase values near the center of the bucket. Such bunch characterized by standard deviation $\sigma_{\rm b} = 0.38\pi$ for parameters chosen for our numerical evaluation that follows, is shown schematically on the Fig. 2(a) by the dotted line. Figure 2(b) shows evolution of resonant particle phase and bucket boundaries with the dc/ac amplitudes ratio. Figure 2 reveals the trade-off in selection of dc/ac ratio. If the ratio is close to one, then virtually no particles will be trapped except the resonant ones, and thus no significant energy transfer to the wave will occur. As dc/ac ratio approaches zero, virtually all particles will be trapped, but energy transfer will approach zero as well. There is an optimum between these two minima, which leads to maximum energy transferred; in our numerical simulation we have chosen a conservative value of 0.2 allowing for trapping of majority of beam particles. The Value of ζ_2 should be dictated by the available potential difference and effects of space charge.

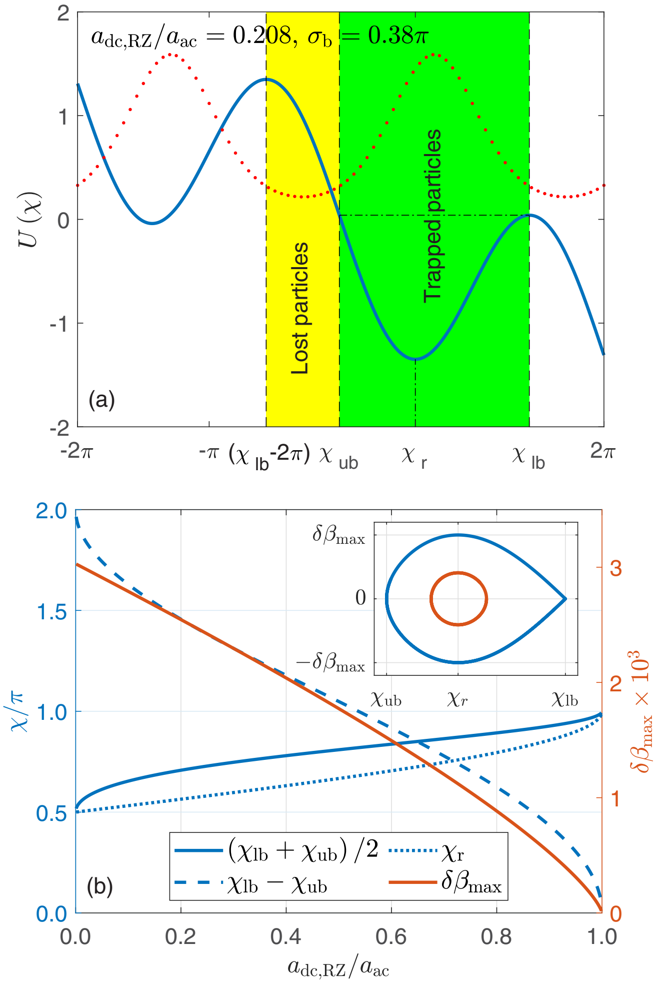

FIG. 2. (a) Normalized potential $U(\chi)$ (solid line) overlapped with FN-bunches charge density in arbitrary units (dotted line). (b) Dependence of bucket properties on the dc to ac ratio in the resonant interaction region. On the inset, trapped particles' trajectories in the phase space: the outer line is the bucket's boundary, the inner circle is the trajectory for a particle relatively close to the resonant particle.

We conclude the discussion regarding the choice of parameters in our model with the DZ, serving as a depressed collector [28]. Up to the sign change, the dc field for this region is found by a procedure virtually identical to the one introduced when we investigated the AZ.

Now that we have established the criteria for choosing the parameters of the quasianalytic and PIC simulations we summarize them in Table I. The simulation was conducted for two sets of parameters applied to identical geometry: (A) providing a negligible space charge and thus low current and low power transfer; (B) optimized to maximise power transfer in expense of increased space charge.

We assume that the dielectric Bragg wave-guide and the periodic structure for frequency and phase velocity of interest, may be designed. Specific implementation of these structures is published elsewhere [29] and is beyond the scope of this

TABLE I. Parameters for numerical verification.

Simulation		A	B	
EM wave frequency	f	1		THz
Cavity length	d	2000		μm
Cavity diameter	$D_{\rm wg}$	100		μm
Vacuum channel diameter	$D_{\rm vc}$	2		μm
Hypothetical diel. const.	$\varepsilon_{\rm slow}$	100		
Cathode position	$d\zeta_{\rm K}$	10	0	μm
Acceleration zone length	$d\zeta_1$	607	532	μm
Deceleration zone length	$d(1-\zeta_2)$	617	519	μm
Normalized phase velocity	$\beta_{\rm ph}$	0.1024		
EM wave amplitude	$E_0^{\rm (ac)}$	-0.24	-3	MV/m
DC field in AZ	$E_0^{\rm (dc,AZ)}$	-4.45	-5.52	MV/m
DC field in RZ	$E_0^{\rm (dc,RZ)}$	-0.05	-0.6	MV/m
DC field in DZ	$E_0^{\rm (dc,DZ)}$	4.15	4.54	MV/m
Static magnetic field	B_z	2		T
Cathode work function	W	5.1		eV
Field enhancement factor	$\beta_{\rm FN}$	1000	674	
Bunch standard deviation	$\sigma_{\rm b}$	0.38	0.155	π
Effective cathode area	$A_{\rm K}$	0.02	0.134	$\mu{\rm m}^2$
Average cathode current	$\langle I_{\rm K}\rangle$	0.9	51.8	μA
Particles-wave power tr.	$P_{\rm p-w}$	0.04	15	mW
Efficiency		24.8	24.2	%

Letter. Thus, the simulated device is a simplified version of the configuration shown in Fig. 1. It is a metallic cylindrical waveguide of length d and diameter $D_{\rm wg}$ filled with a hypothetical dielectric material of dielectric constant $\varepsilon_{\rm slow}$; with virtually identical phase and group velocity as our system requires. Vacuum channel of diameter $D_{\rm vc}$ allows for e-beam passage on the axis of the cylinder. The structure is characterized by a propagating TM mode with cutoff frequency of 0.23 THz and phase velocity $\beta_{\rm ph}$ at 1 THz.

The simplified version of the device considered in PIC simulations serves for validation of quasianalytic formulation and estimation of an order of magnitude for achievable radiation power and efficiency. However, this simplified configuration assumes electromagnetic wave occupying entire cross-section of the device, while in reality all disk-loaded slow-wave structures are characterized by internal radius well below cutoff at the frequency of interest [30]. Therefore, the simplified configuration cannot be used for gain estimation of the device. While ferroelectric materials with epsilon on a scale of few thousands ($BaTiO_3$) are available, strong nonlinear character makes their usage challenging. Therefore, a disk-loaded slow-wave structure of our original configuration, Fig. 1, is preferable.

In Simulation A, field-emission particle point source of effective area $A_{\rm K}$ is located on the cavity axis at $z_{\rm K} = d\zeta_{\rm K}$. For our parameters, this source emits average current $\langle I_{\rm K}\rangle$ on a scale, which may be achieved with a single multiwall CNT [31]. CNT emitter assumed in Simulation B has a diameter of $\sim$0.5 μm. It is simulated as a (temporal) Gaussian point source with parameters calculated from the applied fields according to Ref. [23]. An electromagnetic (EM) wave oscillating at frequency f and with an amplitude $E_0^{\rm (ac)}$ enters the structure at $z = 0$ and leaves it at $z = d$. A uniform dc field ($E_0^{\rm (dc,AZ)}$, $E_0^{\rm (dc,RZ)}$, and $E_0^{\rm (dc,DZ)}$) is imposed in each zone.

The simulation is a self-consistent solution of the EM field and particle dynamics including the nonlinear field emission process [18,23]. We record the particles' phase space coordinates in terms of χ and $\delta\beta$ in several cross-sectional positions along the simulated structure and compare the results with the values achieved for analytical estimation of the FN emission current and integration of equation of motion for the same set of parameters. Results of semianalytical estimation and self-consistent PIC simulation for negligible space charge are shown in Figs. 3(a) and 3(b), respectively (parameters of Simulation A). The similarity between the two is evident. Figure 3(c) shows results of Simulation B considering a nonnegligible current and space charge (pay attention to the difference in $\delta\beta_{\rm max}$ between the two cases). Here, with beam current of 50 μA, space charge causes considerable distortion of the bunches (less particles are trapped) in spite the fact that initial bunch length is much shorter than in case A. However, power transfer from the particles to THz wave is more than two orders of magnitude higher compared to the low-current configuration (due to larger current and fields' values). This result is an evidence for a trade-off between generated THz power and efficiency of the process. In both simulations the efficiency of electromagnetic power generation, calculated as a ratio between the particles to wave power transfer $P_{\rm p\text{-}w}$ and average power delivered by the dc field (product of average current and cathode-anode potential difference) is on a scale of 25%.

In our quasianalytic model and PIC simulations we have considered a *steady-state* regime. While a model for *transient* regime is beyond the scope of this Letter, two options are envisioned: (i) a driven oscillator or amplifier, in which case the signal is launched as a cylindrical wave between two metallic electrodes; (ii) oscillator regime, when ac signal grows out of noise. In the latter case the dc field is increased initially above threshold current of the oscillator. As oscillation starts, the dc is reduced to the equilibrium value. In any case, coupling of the ac field to the cavity is via one or more grooves between the metal disks with Bragg mirror removed.

We have limited our investigation by the case of uniform dc field in the resonant zone and consequently a uniform ac amplitude as required by the equilibrium condition, Eq. (6). Lifting of this limitation would open possibilities for BWO-like configurations, allowing ac amplitude maximum on the cathode while reducing total electromagnetic energy in the cavity. The major difficulty we conceive in this case is an elevated noise level due to the fact that the input is close to the collector. In addition, back propagating wave in the fundamental Floquet harmonic requires smaller period L of the structure and more heat would need to be dissipated due to higher ohm losses.

Our quasianalytic model demonstrates to be in excellent agreement with PIC code. Simulations show possibility of generation of up to 15 mW power with about 25% efficiency at 1 THz from the resonant interaction region of about 0.8 mm length with diameter of the device on a scale of 100 μm at the average cathode current of about 50 μA. Taking in account the cross-sectional dimension of the device, expansion to a

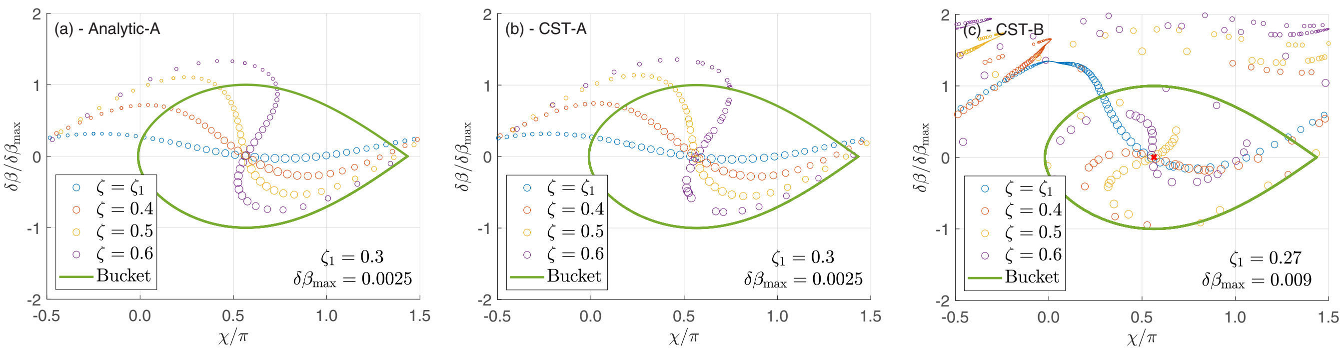

FIG. 3. Evolution of particles' phase space in the RZ, starting from the boundary with AZ at $\zeta = \zeta_1$. Circles' diameter is proportional to charge density of microbunches. (a) Numerical integration of equation of motion for parameters' set of Simulation A. While our treatment is based purely on Newtonian mechanics (justified by low energies involved), this simplification introduces a nonnegligible error in final velocity of the resonant particle. This is straight-forwardly corrected by employing the relativistic kinetic term $\beta_{\text{ph}}^2/2 \rightarrow \gamma_{\text{ph}} - 1$. (b) Results of PIC simulation for the same parameters (space charge effect is negligible). (c) Results of PIC simulation for parameters' set of Simulation B (considerable space charge).

10×10 array, may elevate the generated power by two orders of magnitude in a total volume of few mm^3.

To conclude, we have demonstrated the feasibility of electrostatic tapering such that the net average force of the ac field is compensated by the dc field, which may be interpreted as "direct" energy transfer from the dc to the ac field. This is the main result of our study and it is facilitated by a set-up which consists of a superposition of dc and ac fields in all its three components—e-gun, RZ, and collector. Specifically, we developed a double-periodic structure which consists of dielectric Bragg-mirrors for the radial confinement of the radiation and an array of metallic hollow electrodes imposing a dc field for acceleration (or deceleration) and confinement of the electrons. In addition, the metallic electrodes are designed such that in the longitudinal direction, they control the ac wave phase velocity. According to the results of our analysis, amplification of THz radiation seems feasible, the manufacturing process favors photolithography normally associated with solid state devices which leads to compact implementation. A realistic assessment of the efficiency reveals values characteristic to vacuum tube devices.

This study was supported by the Israel Science Foundation isf 646/18.

[1] T. J. Orzechowski, B. R. Anderson, J. C. Clark, W. M. Fawley, A. C. Paul, D. Prosnitz, E. T. Scharlemann, S. M. Yarema, D. B. Hopkins, A. M. Sessler, and J. S. Wurtele, Phys. Rev. Lett. **57**, 2172 (1986).
[2] R. A. Lewis, J. Phys. D **47**, 374001 (2014).
[3] T. Nagatsuma, IEICE Electr. Express **8**, 1127 (2011).
[4] J. H. Booske, R. J. Dobbs, C. D. Joye, C. L. Kory, G. R. Neil, G.-S. Park, J. Park, and R. J. Temkin, IEEE Trans. Terahertz Sci. Technol. **1**, 54 (2011).
[5] P. H. Siegel, Int. J. High Speed Electr. Syst. **13**, 351 (2003).
[6] T. Kürner and S. Priebe, J. Infrared Milli. Terahz. Waves **35**, 53 (2014).
[7] P. Shumyatsky and R. R. Alfano, J Biomed. Opt. **16**, 033001 (2011).
[8] S. Zhong, Front. Mech. Eng. **14**, 273 (2019).
[9] A. Redo-Sanchez, N. Laman, B. Schulkin, and T. Tongue, J. Infrared, Millimeter, Terahertz Waves **34**, 500 (2013).
[10] G. Scalari, S. Blaser, J. Faist, H. Beere, E. Linfield, D. Ritchie, and G. Davies, Phys. Rev. Lett. **93**, 237403 (2004).
[11] M. Dyakonov and M. Shur, Phys. Rev. Lett. **71**, 2465 (1993).
[12] S. Vainshtein, J. Kostamovaara, V. Yuferev, W. Knap, A. Fatimy, and N. Diakonova, Phys. Rev. Lett. **99**, 176601 (2007).
[13] S. S. Dhillon, M. S. Vitiello, E. H. Linfield, A. G. Davies, M. C. Hoffmann, J. Booske, C. Paoloni, M. Gensch, P. Weightman, G. P. Williams, E. Castro-Camus, D. R. S. Cumming, F. Simoens, I. Escorcia-Carranza, J. Grant, S. Lucyszyn, M. Kuwata-Gonokami, K. Konishi, M. Koch, C. A. Schmuttenmaer *et al.*, J. Phys. D **50**, 043001 (2017).
[14] T. Saito, Y. Tatematsu, Y. Yamaguchi, S. Ikeuchi, S. Ogasawara, N. Yamada, R. Ikeda, I. Ogawa, and T. Idehara, Phys. Rev. Lett. **109**, 155001 (2012).
[15] W. He, C. R. Donaldson, L. Zhang, K. Ronald, P. McElhinney, and A. W. Cross, Phys. Rev. Lett. **110**, 165101 (2013).
[16] P. H. Siegel, A. Fung, H. Manohara, J. Xu, and B. Chang, in *Proceedings of the 12th International Symposium on Space THz Technology, San Diego, CA, paper 3.3*, NASA Technical Reports Server, 2001.
[17] N. de Jonge, M. Allioux, J. T. Oostveen, K. B. K. Teo, and W. I. Milne, Phys. Rev. Lett. **94**, 186807 (2005).
[18] M. Voin and L. Schächter, J. Appl. Phys. **128**, 243303 (2020).
[19] W. Dyke, IRE Trans. Military Electr. **MIL-4**, 38 (1960).
[20] F. Charbonnier, J. Barbour, L. Garrett, and W. Dyke, Proc. IEEE **51**, 991 (1963).
[21] R. H. Fowler and L. Nordheim, Proc. Roy. Soc. London Ser. A **119**, 173 (1928).

[22] L. Schächter and W. D. Kimura, Nucl. Instrum. Methods Phys. Res. Sect. A **875**, 80 (2017).
[23] M. Voin and L. Schächter, in *Proceedings of the ICSEE International Conference on the Science of Electrical Engineering* (IEEE, 2018).
[24] A. Mizrahi and L. Schächter, Phys. Rev. E **70**, 016505 (2004).
[25] L. Schächter, *Beam-Wave Interaction in Periodic and Quasi-Periodic Structures (Particle Acceleration and Detection)*, 2nd ed. (Springer, Berlin, 2011).
[26] C.-C. S. Technology, *Computer Simulation Technology, Studio Suite* (2019).
[27] N. Kroll, P. Morton, and M. Rosenbluth, IEEE J. Quant. Electron. **17**, 1436 (1981).
[28] W. H. Urbanus, W. A. Bongers, V. Bratman, C. A. J. van der Geer, M. F. Graswinckel, P. Manintveld, B. L. Militsyn, and A. Savilov (FEM Team), Phys. Rev. Lett. **89**, 214801 (2002).
[29] M. Voin, THz Radiation Source Based on an Electron Beam in a Double-Periodic Cavity, Ph.D. thesis, The Technion—Israel Institute of Technology, 2021.
[30] E. Kuang, T. J. Davis, G. Kerslick, J. A. Nation, and L. Schächter, Phys. Rev. Lett. **71**, 2666 (1993).
[31] K. B. K. Teo, E. Minoux, L. Hudanski, F. Peauger, J.-P. Schnell, L. Gangloff, P. AU Legagneux, D. Dieumegard, G. A. J. Amaratunga, and W. I. Milne, Nature (London) **437**, 968 (2005).